### RESEARCH ARTICLE



WILEY

Check for updates

# Effects of *Tulp4* deficiency on murine embryonic development and adult phenotype

Roland Jäger<sup>1</sup> | Stefan H. Geyer<sup>2</sup> | Anoop Kavirayani<sup>3</sup> | Máté G. Kiss<sup>1</sup> | Elisabeth Waltenberger<sup>4</sup> | Thomas Rülicke<sup>5,6</sup> | Christoph J. Binder<sup>1</sup> | Wolfgang J. Weninger<sup>2</sup> | Robert Kralovics<sup>1</sup>

### Correspondence

Stefan H. Geyer, Division of Anatomy, Center for Anatomy and Cell Biology, Medical Imaging Cluster, Medical University of Vienna, Waehringer Str. 13, 1090 Vienna, Austria. Email: stefan.geyer@meduniwien.ac.at

### Funding information

Austrian Science Fund Projects, Grant/Award Numbers: P29018-B30, F4702-B20

Review Editor: Alberto Diaspro

### **Abstract**

Genetically engineered mouse models have the potential to unravel fundamental biological processes and provide mechanistic insights into the pathogenesis of human diseases. We have previously observed that germline genetic variation at the TULP4 locus influences clinical characteristics in patients with myeloproliferative neoplasms. To elucidate the role of TULP4 in pathological and physiological processes in vivo, we generated a Tulp4 knockout mouse model. Systemic Tulp4 deficiency exerted a strong impact on embryonic development in both Tulp4 homozygous null (Tulp4-/-) and heterozygous (Tulp4+/-) knockout mice, the former exhibiting perinatal lethality. High-resolution episcopic microscopy (HREM) of day 14.5 embryos allowed for the identification of multiple developmental defects in Tulp4-/- mice, including severe heart defects. Moreover, in Tulp4+/- embryos HREM revealed abnormalities of several organ systems, which per se do not affect prenatal or postnatal survival. In adult Tulp4+/- mice, extensive examinations of hematopoietic and cardiovascular features, involving histopathological surveys of multiple tissues as well as blood counts and immunophenotyping, did not provide evidence for anomalies as observed in corresponding embryos. Finally, evaluating a potential obesity-related phenotype as reported for other TULP family members revealed a trend for increased body weight of Tulp4+/- mice.

### Research Highlights

- To study the role of the *TULP4* gene *in vivo*, we generated a *Tulp4* knockout mouse model.
- Correlative analyses involving HREM revealed a strong impact of *Tulp4* deficiency on murine embryonic development.

### KEYWORDS

histopathology, HREM, knock out mouse model, perinatal lethality, phenotypic assay

Wolfgang J. Weninger and Robert Kralovics contributed equally to this work and share senior authorship.

This is an open access article under the terms of the Creative Commons Attribution License, which permits use, distribution and reproduction in any medium, provided the original work is properly cited.

© 2023 The Authors. Microscopy Research and Technique published by Wiley Periodicals LLC.



<sup>&</sup>lt;sup>1</sup>Department of Laboratory Medicine, Medical University of Vienna, Vienna, Austria

<sup>&</sup>lt;sup>2</sup>Division of Anatomy, Center for Anatomy and Cell Biology, Medical Imaging Cluster, Medical University of Vienna, Vienna, Austria

<sup>&</sup>lt;sup>3</sup>Vienna BioCenter Core Facilities GmbH, Austrian BioImaging/CMI, Vienna, Austria

<sup>&</sup>lt;sup>4</sup>CeMM Research Center for Molecular Medicine of the Austrian Academy of Sciences, Vienna, Austria

<sup>&</sup>lt;sup>5</sup>Department of Biomedical Sciences, University of Veterinary Medicine Vienna, Vienna, Austria

<sup>&</sup>lt;sup>6</sup>Ludwig Boltzmann Institute for Hematology and Oncology, Medical University of Vienna, Vienna, Austria

### 1 | INTRODUCTION

Myeloproliferative neoplasms (MPN) are a group of chronic hematologic malignancies characterized by elevated production of different types of blood cells. Thrombosis is a major complication in MPN, influenced by genetic factors. Our previous work based on genome-wide association studies (GWAS) provided evidence for a haplotype at the chromosomal locus 6g25.3 to confer increased risk for arterial thrombosis in MPN patients. Moreover, we could demonstrate that presence of the 6q25.3 risk variants influences transcriptional regulation of the TULP4 gene (Jäger et al., 2015). TULP4 encodes a member of the family of tubby-like proteins (TULPs), encompassing TUB as well as TULP1, TULP2, TULP3, and TULP4. The TULP founding member TUB was implicated in a spontaneous maturityonset obesity syndrome in mouse strains, caused by a recessive loss-of-function mutation in the TUB gene (Coleman & Eicher, 1990; Kleyn et al., 1996; Noben-Trauth et al., 1996). Functional studies on TUB. TULP1 and TULP3 revealed a role in ciliary function thereby affecting energy balance, neural development and function, photoreception, and hearing. Furthermore, TULPs have a role in endocytosis, phagocytosis and synapse maintenance, or architecture (Mukhopadhyay & Jackson, 2011; Wang et al., 2018). Mutations in TULP1 were described in retinitis pigmentosa (Banerjee et al., 1998; Gu et al., 1998; Hagstrom et al., 1998), and TULP3 was shown to play a role in sonic hedgehog signaling during mouse embryonic development (Patterson et al., 2009). Data published on TULP2 and TULP4 are restricted to expression profiling and in vitro molecular characterization (Mukhopadhyay & Jackson, 2011). Sequence alignment in conjunction with domain mapping allowed for the determination of evolutionary relationships within TULPs that suggested TULP1-3 to be closely related, whereas TULP4 is more distant (Li et al., 2001; North et al., 1997). While TULPs other than TULP4 have been to partly characterized in respect of their mechanistic role in cellular signaling, knowledge on TULP4 function is scarce. To evaluate the role of the TULP4 gene in thrombosis and beyond, we generated an in vivo model for Tulp4 deficiency in the form of a novel Tulp4 knockout mouse. We intended to use this model to perform extensive phenotyping of Tulp4 deficiency with respect to the hematopoietic system.

Early attempts to breed both *Tulp4* homozygous null (*Tulp4*—/—) and *Tulp4* heterozygous (*Tulp4*+/—) knockout mice suggested perinatal lethality in *Tulp4*—/— mice. To elucidate the mechanisms underlying the lethality phenotype, we sought to unravel the impact of *Tulp4* deficiency on embryonic development. To achieve this, we applied high-resolution episcopic microscopy (HREM) as an approach complementary to standard histopathology methods. HREM is a block-face scanning method, based on automated physical sectioning of resinembedded samples while producing series of images from the freshly exposed block surface (Weninger et al., 2006, 2018). The images can be virtually stacked to produce three-dimensional (3D) volume data in near histologic image quality. Thus, by processing whole mouse embryos, HREM permits identification of small as well as large structural abnormalities of tissues and organs (Wendling et al., 2021; Weninger

et al., 2014). This ensures an unbiased and comprehensive systematic evaluation of the full range of malformations in novel mouse knockout lines that might bear unknown anatomical defects. For this reason, HREM had been established as one of the key imaging technologies for large-scale phenotyping studies of pre- or perinatal lethal mouse lines (Adams et al., 2013; Mohun et al., 2013) and was used to identify gene function in selected lines (De Franco et al., 2019; Ghadge et al., 2021; Mohun et al., 2013). Physical resin-sections produced during HREM-data generation can be collected and used for further light microscopic assessment. This allows for subsequent selective histopathologic analysis (Zopf et al., 2021).

Making use of HREM in conjunction with correlative histopathologic analyses allowed us to investigate the lethality phenotype observed in Tulp-/- and the range of minor defects in Tulp4+/- embryos. Based on the results derived from this integrative imaging approach, we subsequently extended our phenotyping efforts onto adults.

### 2 | MATERIALS AND METHODS

### 2.1 | Generation of a *Tulp4* knockout mouse strain

To generate an in vivo model for Tulp4 deficiency, we have used commercially available genetically engineered mouse embryonic stem (ES) cells carrying a targeted *Tulp4* allele (TULP4<sup>tm1a(KOMP)Wtsi</sup>: mutant cell line EPD0112\_4\_G12) from the knockout mouse project (KOMP) repository, provided through the international mouse phenotyping consortium (IMPC). The ES cell clone carrying a knockout-first allele was generated through insertion of an L1L2 Bact P cassette at position 6.256,719 (build GRCm39) of mouse chromosome 17 upstream of Tulp4 exon 6. The cassette is composed of a mouse engrailed 2 splice acceptor (En2 SA), lacZ, a neomycin resistance gene as well as FRT and loxP sites (Supplementary Figure S1). The resulting targeted Tulp4 allele is predicted to result in a non-expressive form owing to the in-frame fusion of lacZ by the En2 SA. Using the fully verified targeted ES cells derived from the C57BL/6N strain, founder chimeric mice were generated through microinjection into BALB/c blastocysts. Animal experiments have been approved by the Ethics and Animal Welfare Committee of the University of Veterinary Medicine Vienna in accordance with the University's guidelines for Good Scientific Practice and authorized by the Austrian Federal Ministry of Education, Science and Research (BMWF-68.205/0023-II/3b/2014) in accordance with current legislation. Chimeras were then bred with C57BL/6NRj mice to generate germline transmitting Tulp4 deficient mice heterozygous for the Tulp4 knockout allele (i.e., Tulp4+/-). ES cell-based gene targeting using the knockout-first strategy was developed to create a multipurpose allele for both knockout and conditional applications (Skarnes et al., 2011). In the present study, we used only systemic, whole-body knockout mice to investigate the effect of systemic Tulp4 deficiency. The novel Tulp4 knockout strain was deposited to the European Mouse Mutant Archive (EMMA) repository under accession number EM:10971 (https://www.infrafrontier.eu/ emma/).

### 2.2 | Mouse genotyping, breeding, and maintenance

Genotyping of embryos and pups was performed by polymerase chain reaction (PCR) using primer pairs listed in Supplementary Table S1. Presence of a knockout allele was evaluated through PCR-based detection of the knockout-first cassette inserted 5' as well as the adjacent loxP site inserted 3' of Tulp4 exon 6 (Supplementary Figure S1) using primer pairs "knockout cassette" and "knockout loxP" (Supplementary Table S2). Presence of a wildtype allele was evaluated by successful amplification of a 380 base pair product spanning the cassette insertion site, the latter precluding the generation of a PCR product (primer pair "wildtype"; Supplementary Table S2 and Supplementary Figure S1). Mouse breeding and maintenance was performed at the animal facility of the Institute of Molecular Biotechnology Austria, Vienna, which is run as full barrier mouse husbandry provided with HEPA filtered air (15x air exchange rate per hour). Mice were maintained in ventilated cages on autoclaved standard pelleted diet (SSNIFF) and acidified autoclaved water (pH 2.5-3.0). Mouse breeding was performed in accordance with the respective license approved by the institutional and national ethical committees (animal protocol GZ: 311633/2014/9, approved by the City of Vienna (Austria)).

### 2.3 | High-resolution episcopic microscopy

Mouse dams were sacrificed by cervical dislocation on day 14.5 post conception and embryos were dissected from the uterus. They were further transferred to phosphate buffered saline (PBS) at 37°C and the amnion was carefully removed under a stereomicroscope. After that, embryos were fixed in 4% paraformaldehyde (PFA) in PBS on a shaker at 4°C for at least 24 h. Embryos were then processed routinely for HREM (Geyer, Maurer-Gesek, Reissig, & Weninger, 2017; Mohun & Weninger, 2012a, 2012b). Briefly, samples were dehydrated in increasing concentrations of ethanol (70%, 80%, 90%, 95%, 100%) for 2-4 h in each step. Following dehydration, embryos were infiltrated with JB-4 (Polysciences Inc., Warrington, PA, United States) containing 0.4 g eosin B per 100 mL for 48-72 h, embedding solution was changed twice. The samples were then embedded in eosin-dyed resin JB-4 (0.4 g eosin per 100 mL embedding solution). JB-4 blocks were sealed to allow for polymerization in an oxygen-free surrounding for 24 h at room temperature. Hardened blocks were baked at 90°C for 24-48 h. Digital volume data of whole embryos were generated using an optical-HREM apparatus (Indigo Scientific Ltd., Baldock, UK). During sectioning, physical sections were captured to be processed for later histopathologic examinations. The HREM images were downscaled to gain isotropic voxel sizes of 3 µm<sup>3</sup> and stacked to produce digital volume data. Volume renderings of the embryo surfaces were produced and employed for identifying the precise developmental stage according to the system proposed by Geyer, Reissig, Rose, et al. (2017) for E14.5 embryos. Finally, the phenotype was carefully and systematically analyzed using the software packages Amira and OsiriX

following established phenotyping protocols (Geyer, Reissig, Rose, et al., 2017; Weninger et al., 2014).

### 2.4 | Classical histopathology on mouse embryos and newborns

To investigate possible micro-pathologies triggering the observed perinatal lethality, nine E17.5 embryos (3 Tulp4+/+, 3 Tulp4+/-, and 3 Tulp4-/-) and one deceased PO newborn (Tulp4-/-) were submitted for histopathological analysis. Whole-body E17.5 and P0 were fixed by immersion in 10% neutral buffered formalin for 48 h, processed with a logos automated tissue processor (milestone medical), and embedded in paraffin. Sagittal and parasagittal sections of the embryos were prepared with a standard rotary microtome (Microm HM 355, Thermoscientific) and the sections were stained with hematoxylin and eosin (HE) using the automated HMS 740 stainer (Gemini AS). The stained sections were examined by a board certified veterinary anatomic pathologist with experience in comparative laboratory animal pathology using a Zeiss Axioskop MOT 2 microscope. Selected sections were digitized using the Pannoramic Flash 250 III whole slide scanner (3D Histech) with the 20× plan apochromat objective and the Adimec Quartz Q12A180fc camera. Microscopic images were acquired with a spot insight microscope camera (Spot Imaging, Diagnostic Instruments). Whole slide images (scans) were reviewed, and additional static images were acquired from the scans, with the Case-Viewer™ software (3D Histech). The collected HREM sections were processed following an routine HE staining protocol (Zopf et al., 2021).

### 2.5 | Phenotyping of adult *Tulp4+/-* mice

Upon euthanasia, mice were subjected to routine necropsy examination and dissected. Representative samples of relevant organs were prepared and a series of examinations was performed, including histopathological analysis and immunophenotyping. Details on phenotyping efforts in adult Tulp4+/- mice are provided in the Supplementary methods.

### 2.6 | Body weight phenotypic assay

To validate spontaneous observations on increased body-weight in adult Tulp4+/- mice, we conducted a large weighting series under controlled conditions. Several mating trios (Tulp4+/- females/males with Tulp4+/+ mating partners) were set up specifically for the experiment, resulting in a large number of litters delivered within a time span of 8 days. This allowed for setting up a total of 19 cages (7 female cages, 12 male cages) for subsequent follow-up of body weight. Each matched cage contained four mice of same sex and age, two Tulp4+/- and two Tulp4+/+ mice. Experimental cages were maintained

**TABLE 1** (A) Observed *Tulp4* genotype rates as compared with expected percentages based on Mendelian laws; (B) Observed *Tulp4* genotype rates in embryonic stages E14.5 and E17.5, and after birth (P0).

(A)	Observed	Expected	
Total offspring	30	n.a.	
Tulp4+/+	11 (35%)	7.5 (25%)	
Tulp4+/-	19 (61%)	15.0 (50%)	
Tulp4-/-	1 (3%)	7.5 (25%)	p = .018
(B)	E14.5	E17.5	P0
Litter size	10 (100%)	9 (100%)	7 (100%)
Tulp4+/+	2 (20%)	3 (33%)	2 (29%)
Tulp4+/-	7 (70%)	3 (33%)	4 (57%)
Tulp4-/-	1 (10%)	3 (33%)	1 (14%)

on standard conditions and regular diet. Weight was measured every 1–4 weeks for a time span of 66 weeks. In three cages, one mouse each died as commonly observed under standard maintenance. These cages were subsequently omitted. Only cages with four healthy mice followed up for the full observation time of 66 weeks were included in the analysis, which applied to a total of 16 cages (6 female cages, 10 male cages corresponding to 24 female mice and 40 male mice at balanced genotype ratios). Weighting was performed on exact time points with respect of dates of birth, with an imprecision of maximum 2 days (no follow-up on weekends), starting at week three after birth.

### 2.7 | Statistical analyses

Statistical evaluation of observed genotype frequencies as compared to expected Mendelian ratios was performed using a chi-square goodness-of-fit test. For analysis of immunophenotyping data, lymphocyte subsets from different genotypes (Tulp4+/- vs. Tulp4+/+) were compared using an unpaired t-test. In the body weight phenotypic assay, weight differences for single observations were evaluated using an unpaired t-test, whereas longitudinal weighting data were analyzed applying two-way ANOVA followed by Sidak's multiple comparison test. All statistical testing was performed using the GraphPad Prism software.

### 3 | RESULTS

### 3.1 | Tulp4-/- offspring are not viable

To generate both Tulp4+/- and Tulp4-/- offspring, the latter being homozygous for the knockout allele, heterozygous mating trios were set up for breeding. While the expected percentage of Tulp4-/- offspring is 25% according to Mendelian laws, initial observations on litters from heterozygous breeding indicated a strongly reduced frequency of Tulp4-/- offspring 7 days after birth, when tissue

biopsies for genotyping were taken. Specifically, a total of eight litters yielded in 31 pups, 11 (37%) of which were wildtype for Tulp4 (Tulp4 +/+), 19 (63%) were Tulp4+/-, and one single pup (3%) was Tulp4—/—. The latter pup was observed alive but sick and small in size, and was therefore sacrificed on day seven after birth. Statistical evaluation of observed over expected genotype frequencies based on Mendelian ratios suggested a perinatal lethal phenotype of Tulp4 deficiency (p = .018; Table 1a). As the observation of one alive Tulp4-/pup precluded a fully penetrant embryonic lethality phenotype, timecontrolled mating was set up to determine the exact genotype ratios at two embryonic stages (E14.5 and E17.5) and at birth (P0), the latter involving close observation of pregnant females around the day of expected delivery. Tulp4-/- were found in both embryonic stages evaluated, as well as at P0 (Table 1b). Of note, in the P0 litter only one of seven pups was Tulp4-/-. The Tulp4-/- newborn was observed dead after birth at PO. Interestingly, necropsy examination of the Tulp4-/- P0 pup revealed the presence of meconium in the large intestine (Figure 1a), indicating a functionally intact digestive system at birth (Jerdee et al., 2015; Skelly et al., 2022).

## 3.2 | Histopathological sections of *Tulp4*-/- whole E17.5 embryos and P0 neonates do not reveal morphological abnormalities

To identify anatomic and histologic correlates for the observed perinatal lethality, a histopathological workup was performed on late-stage embryos (E17.5) as well as on newborn pups (P0). Specifically, a total of 15 E17.5 embryos (3 *Tulp4+/+*, 7 *Tulp4+/-*, and 5 *Tulp4-/-*) and seven P0 neonates (2 *Tulp4+/+*, 4 *Tulp4+/-* and 1 *Tulp4-/-*) were reviewed for the presence of anatomical and histological abnormalities. Light microscopic evaluation of two-dimensional (2D) sagittal and parasagittal sections revealed no cranial, thoracic, or abdominal malformations in these subsets of embryos. The brain, spinal cord, thoracic organs (including heart and lung), and abdominal organs (including liver and intestines) did not show evidence of significant developmental malformations at light microscopic level (Figure 1b).

### 3.3 | HREM identifies severe developmental defects in *Tulp4*—/— mouse E14.5 embryos

To overcome limitations of classical histopathological analysis, we made use of HREM to generate 3D volume data sets from four Tulp4-/- mouse embryos in conjunction with five Tulp4+/+ littermates. The HREM survey identified severe anatomical malformations in all four Tulp4-/- embryos. Notably, all of them exhibited significant abnormalities of the cardiovascular system. In three embryos, cardiovascular abnormalities included severe malformations of the heart, such as double outlet right ventricle (DORV) ((2/4)), muscular ventricular septal defect (mVSD) (1/4), perimembranous ventricular septal defect (pVSD) (1/4), and bicuspid aortic valve (1/4) (Figure 2). Other vascular abnormalities involved head arteries, where we found

**FIGURE 1** Histopathological evaluation in E17.5 embryos and P0 neonates. (a) Meconium (\*) as found in the large intestine of both Tulp4 homozygous null (Tulp4-/-) and their wildtype littermates (Tulp4+/+) in pups at postnatal (P0) necropsy examinations. (b) Light microscopic evaluation of two-dimensional sagittal and parasagittal sections of E17.5 Tulp4-/- and Tulp4+/+ wildtype littermates.

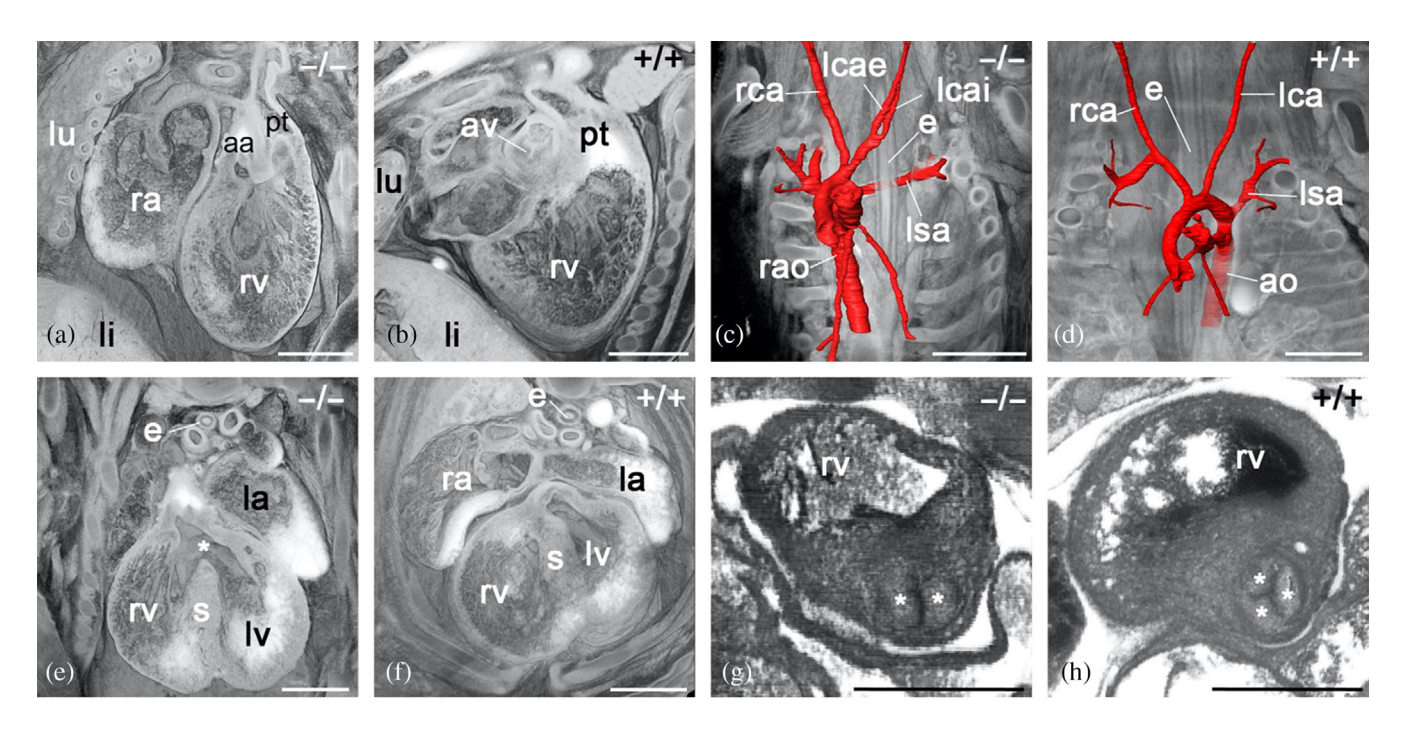


FIGURE 2 Cardiovascular malformations in E14.5 *Tulp4*—/— embryos. (a) Double outlet right ventricle. Volume rendered, virtually sectioned three dimensional (3D) model of heart region from cranio-ventral. (b) Control. (c) Right sided aorta, retroesophageal left subclavian artery, and abnormal origin of left external carotid artery. Surface rendered model of blood vessels in combination with virtually sectioned 3D model. View from ventral. (d) Control. (e) Perimembraneous ventricular septal defect (asterisk). Axial section through volume rendered model, view from cranial. (f) Control. (g) Bicuspid aortic valve, leaflets marked with asterisks. Virtual HREM section view from ventro-lateral. (h) Control. aa, ascending aorta; av, aortic valve; e, esophagus; la, left atrium; lca, left common carotid artery; leca, left external carotid artery; li, liver; lica, left internal carotid artery; lsa, left subclavian artery; lu, lung; lv, left ventricle; pt, pulmonary trunk; rao, right sided aorta; rca, right common carotid artery; ra, right atrium; rv, right ventricle; s, ventricle septum; scale bars = 500 μm.

evidence for dilatations in conjunction with thin vessel walls (4/4), as well as liver vessels, which showed an abnormal hepatic vein connection (1/4) and absence of the ductus venosus valve (1/4). One embryo

(*Tulp4*—/— hom1) exhibited complex malformations of the intrathoracic and cranial arteries, such as a right sided aortic arch, a retroesophageal left subclavian artery, an abnormal external carotid artery

running parallel with the internal carotid artery over a longer distance, abnormal topology of the left intracranial vertebral artery, a hypoplasia of the left stapedial artery, and a missing segment of the right posterior cerebral artery (Figure 2). In addition to the vascular abnormalities, three of the four embryos also showed morphologic abnormalities affecting endocrine or exocrine glands. Two embryos (*Tulp4*—/— hom3 and hom4) showed abnormal thymus topology, and two embryos exhibited abnormal morphology of the thyroid gland (abnormal thyroid gland isthmus morphology [*Tulp4*—/— hom2] and small left lobe of thyroid gland [*Tulp4*—/— hom3]) (data not shown).

## 3.4 | Histomorphological analysis confirms and complements HREM-based observations in *Tulp4*—/—mouse E14.5 embryos

To take advantage of complementary features of HREM and histopathology as demonstrated recently (Keuenhof, Heimel, et al., 2021), we

applied a correlative approach by using the 3D spatial information from HREM to select relevant tissue sections for a 2D workup to gain a view onto cellular details. Specifically, for one of the Tulp4-/-E14.5 embryos (Tulp4-/- hom1) a subset of JB4 sections was collected during HREM data generation. The sections were stained with HE, microscopically examined, and correlated with the HREM observations. Overall, regional macro-morphologic anomalies such as the right sided aortic arch were not represented in the 2D histology images or were not selected for representation, as 3D reconstruction implemented in HREM was considered superior for visualization of such large anomalies. Nevertheless, histopathology allowed for assessing morphology at cellular level in several selected regions (Figure 3). Notably, histopathology findings on the available slides complement some of the observations made with HREM. Specifically, in the cardiovascular system morphologic features strongly suggestive of a double outlet right ventricle/right aortic arch are evident. Valve leaflets and endocardial stroma were within normal limits. Furthermore, 2D sections of the liver revealed normal parenchymal cellularity (Figure 3).

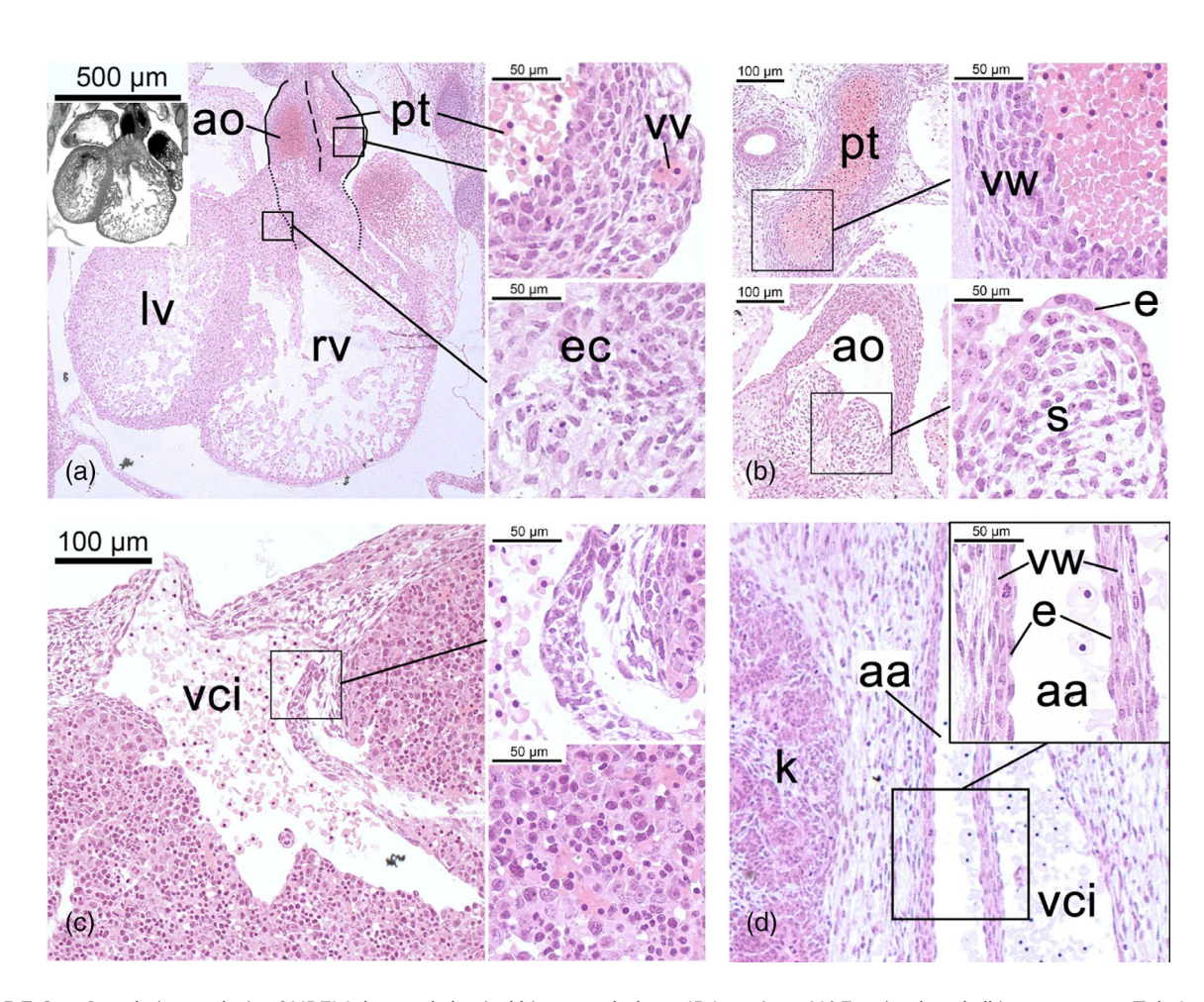


FIGURE 3 Correlative analysis of HREM data and classical histomorphology. JB4 sections, H&E stained, and all images mouse Tulp4—/— (hom1). (a) Heart region. Ascending aorta and pulmonary trunk are strongly indicative of a double-outlet right ventricle. Arterial wall with vasa vasorum and atrioventricular endocardial cushion appear histologically normal. Corresponding HREM image (inlay). (b) Ascending aorta and pulmonary trunk. Vascular wall, Valvular stroma, and valvular endocardium appear histologically normal (right panels). (c) Liver. Intrahepatic part of vena cava inferior. The liver parenchyma is of normal cellularity (right panels). (d) Abdominal aorta. Vessel wall of abdominal aorta is histologically normal. aa, abdominal aorta; ao, ascending aorta; e, endothelium; ec, endocardial cushion; k; kidney; lv, left ventricle; pt, pulmonary trunk; rv, right ventricle; s, valvular stroma; vci, vena cava inferior; ve, valvular endocardium; vv, vas vasis; vw, vessel wall.

10970029, 2024, 4, Downloaded from https:

Universität Wien, Wiley Online Library on [09/07/2025]. See the Terms

observed anomalies therefore being restricted to the macro-morphologic level as detected by HREM.

## 3.5 | HREM identifies developmental defects also in *Tulp4+/-* mouse E14.5 embryos

While perinatal lethality triggered our investigations in Tulp4-/embryos, we did not observe any obvious phenotypic anomalies in Tulp4+/- embryos. Birth rates were within the range expected by Mendelian law, and Tulp4+/- adults appeared normal as their wildtype Tulp4+/+ littermates. Based on the observation of severe morphological anomalies in all four Tulp4-/- E14.5 surveyed, we used HREM to analyze a total of seven Tulp4+/- E14.5 for anatomic and macro-morphologic anomalies, as compared to a set of five E14.5 Tulp4+/+ littermates in conjunction with stage-matched reference data. Overall, anomalies were detected in six of the seven Tulp4+/-. While anatomic anomalies were observed in several organ systems. the most common were abnormalities affecting the vascular system. Specifically, Tulp4+/- embryos exhibited abnormal morphology of the head arteries or the vertebral artery (4/7), telangiectasia (1/7), a blood-filled cyst in the lung (1/7), as well as anomalies related to the venous system such as abnormal liver vasculature (5/7) and dual inferior vena cava (2/7) embryos (Figure 4). Besides the anomalies that can be assigned to the vascular system, two embryos exhibited

abnormalities affecting the infrahyoid muscles and two embryos exhibited a missing connection between the subcutaneous lymph vessels and lymph sacs in conjunction with subcutaneous edema. One embryo each exhibited a thin hypoglossal nerve unilaterally (Tulp+/- het5), abnormal rib development (Tulp+/- het7) (Figure 4), and abnormal testis tissue architecture (Tulp+/- het7) (data not shown). Of note, in one Tulp4+/- embryo our HREM analysis did not identify any abnormalities (Figure 5).

## 3.6 | Developmental defects as observed in *Tulp4* +/- mouse embryos are not reflected in *Tulp4*+/- adult mice

To investigate a potential impact of anatomic defects detected in Tulp4+/- embryos on birth rates and survival, we analyzed genotype distributions in offspring of mixed breeding. According to Mendelian laws, crossing of Tulp4+/- with Tulp4+/+ mice shall result in an equal Tulp4+/- to Tulp4+/+ offspring ratio (50% each). We determined genotypes in mice from 47 litters, delivered over one full year during standard maintenance of the Tulp4 knockout strain, comprising 319 mice (156 females and 163 males). Of the total offspring, 50.8% was Tulp4+/- and 49.2% was Tulp4+/+, suggesting no impact of defects described in Tulp4+/- embryos on birth rates (Table 2). Moreover, follow-up of 64 mice (24 females and 40 males) in a

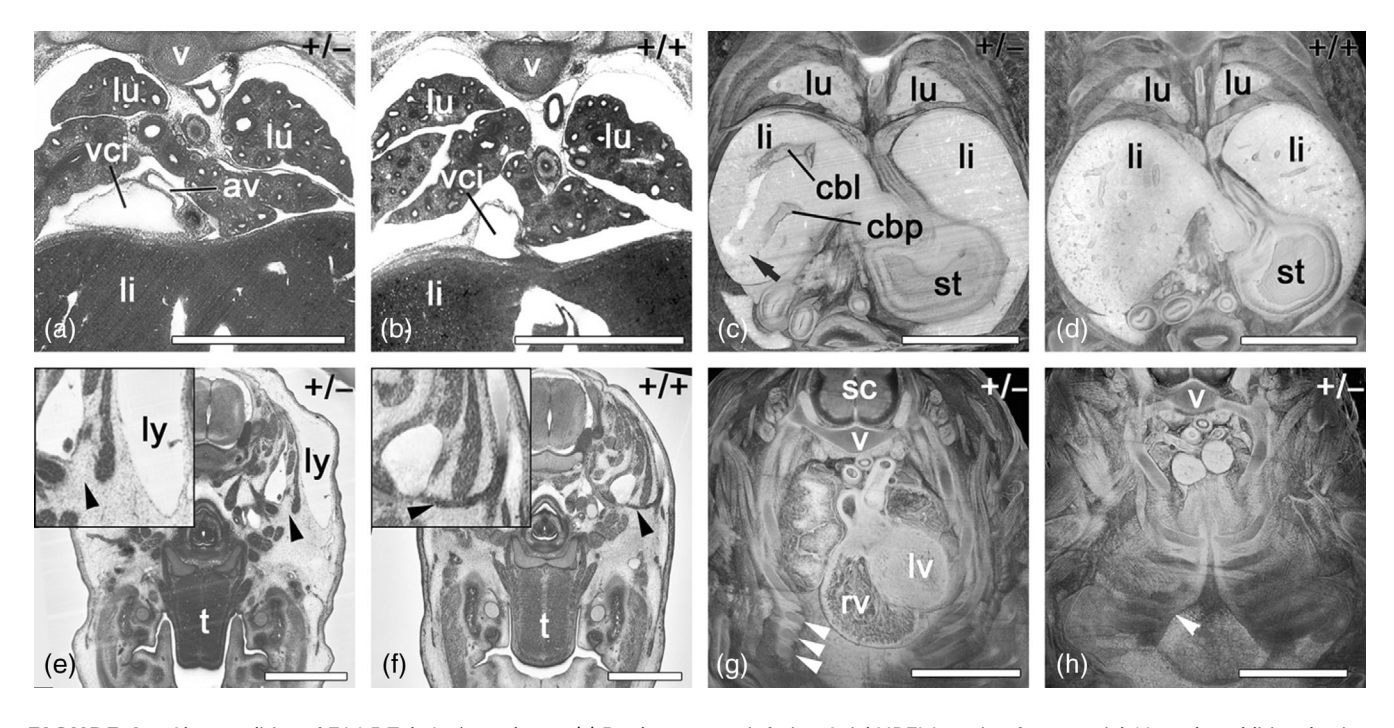


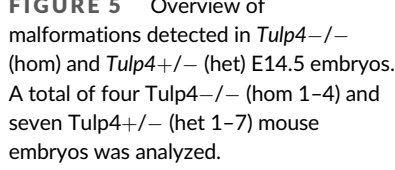
FIGURE 4 Abnormalities of E14.5 *Tulp*4+/- embryos. (a) Dual vena cava inferior. Axial HREM section from cranial. Note the additional vein (av). (b) Control. (c) Abnormal connection of branches of right liver and portal vein (arrow). (d) Control. (e) Missing connection between subcutaneous vessels and left lymph sac (black arrowhead). (f) Control with blood filled connection (black arrowhead). Axial HREM sections from cranial. (g, h) Sternal malformation. Abnormal morphology of sternal ridge (white arrowheads). Volume rendered model, from cranial, (g) and ventral (h). cbl, communicating branch of liver vein; cbp, communicating branch of portal vein; li, liver; lv, left ventricle; lu, lung; ly, lymph vessel; rv, right ventricle; sc, spinal cord; st, stomach; t, tongue; v, vertebra; vci, vena cava inferior; Scale bars = 1000 μm.

10970029, 2024, 4, Downloaded from https://analytical

onlinelibrary.wiley.com/doi/10.1002/jemt.24476 by Vete

he Universität Wien, Wiley Online Library on [09/07/2025]. See the Terms

on Wiley Online Library for rules of use; OA articles are governed by the applicable Creative Commons



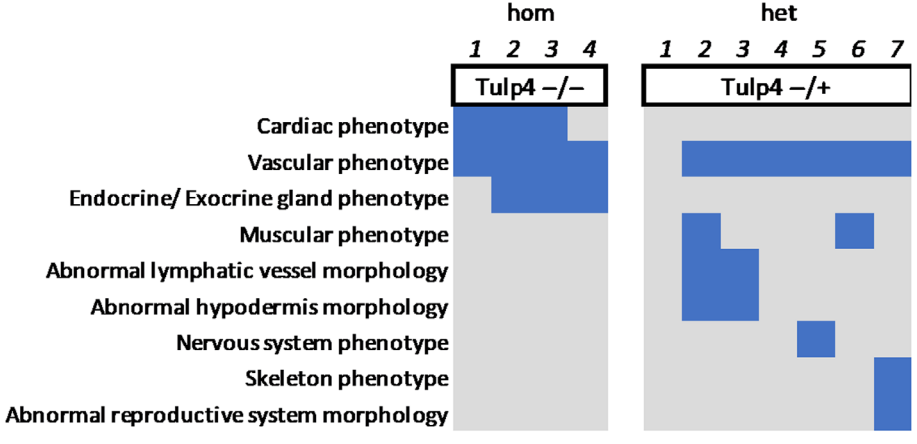


**TABLE 2** Observed versus expected fraction of *Tulp4* heterozygous (Tulp4+/-) offspring arising from regular breeding (Tulp4+/- with Tulp4+/+).

	Observed	Expected
Total offspring	319	n.a.
Total female offspring	156	n.a.
Total male offspring	163	n.a.
Total Tulp4+/+	157 (49%)	159.5 (50%)
Total Tulp4+/-	162 (51%)	159.5 (50%)
Tulp4+/+ females	87 (56%)	78 (50%)
Tulp4+/- females	69 (44%)	78 (50%)
Tulp4+/+ males	70 (43%)	81.5 (50%)
Tulp4+/- males	93 (57%)	81.5 (50%)

controlled setting (four mice per cage at balanced genotype ratio) over a total of 66 weeks did not indicate decreased survival of Tulp4+/- mice.

To evaluate adult mice for a possible manifestation of anatomical malformations as observed in Tulp4+/- embryos, we applied histopathological methods to screen for abnormalities on organ, tissue, and cellular level. Of note, size limitations preclude HREM-based wholebody scans in adult mice. Therefore, relevant organs were harvested from 12 mice (three female Tulp4+/- and three age-matched Tulp4 +/+ females, three male Tulp4+/-, and three age-matched Tulp4+/-+ males) and submitted for histopathological analysis (Supplementary Table S3). To the extent investigated, no abnormalities were observed in Tulp4+/- mice as compared to age- and sex-matched Tulp4+/+ mice (Supplementary Figure S2). Since we generated the Tulp4 knockout mouse based on hypotheses relating to the genetic association of the human 6q25.3 (TULP4) chromosomal locus with a thrombosis phenotype in an MPN patient cohort (Jäger et al., 2015), we used a cohort of 12 mice to specifically evaluate hematopoietic and cardiovascular features. Automated blood count measurements of standard blood parameters as well as morphological examinations of blood smears, bone marrow brush smears, and bone sections (femur, representing a long bone, and sternum; representing a flat bone) did not provide evidence for aberrant hematopoiesis. Immunophenotyping of peripheral

blood and bone marrow confirmed the absence of quantitative differences in leukocytes and leukocyte subsets (Supplementary Figure S3). In histological sections of the unchallenged aorta, there was no evidence for thrombosis or vascular disease. In blood vessels of different organs (including lung, liver, and spleen) and in sections of the heart and aortic valves there was no evidence of blood clots, anatomical abnormalities, or vascular defects at cellular level (Supplementary Figure S2 and Supplementary Table S3). While epidemiologic data on MPN patients suggested TULP4 as a candidate gene for altered risk of arterial thrombosis, no association with venous thromboembolism was observed (Jäger et al., 2015). Major arterial events such as myocardial infarction and stroke frequently arise as a consequence of chronic atherosclerosis, a multifactorial disease with a strong immunological component (Libby et al., 2019). Extensive flow-cytometry based phenotyping of immune cells derived from different organs (Tables S4 and S5) did not reveal any immunological abnormalities in Tulp4+/- adult mice. More specifically, immunophenotyping of peripheral blood as well as bone marrow cells did not provide evidence for quantitative differences of leukocytes subsets between Tulp4+/- mice and Tulp4+/+ littermates (Supplementary Figure S3).

### 3.7 | Increased body weight observed in adult Tulp4+/- mice

The Tub gene, coding for the founding member of the TULP family of proteins, was identified through positional cloning based on a causative mutation for a spontaneous maturity-onset obesity syndrome observed in mouse strains (Noben-Trauth et al., 1996). This led us to hypothesize on a potential obesity-related phenotype also in our Tulp4 knockout mice. In accordance with that, upon initiating breeding of the Tulp4 knockout line, observations on several independent litters suggested a trend for increased body weight in Tulp4 +/females aged 4-7 months (Figure 6a). Of note, the observed trends did not reach formal statistical significance. These observations were noted postmortem prior to organ harvests, precluding follow-up weight measurements in those litters. To follow up on the initial observations, we specifically set up weighting experiments under

10970029, 2024, 4, Down

om/doi/10.1002/jemt.24476

Universität Wien, Wiley Online Library on [09/07/2025]. See the Terms

on Wiley Online Library for rules of use; OA articles are governed by the applicable Creative Common

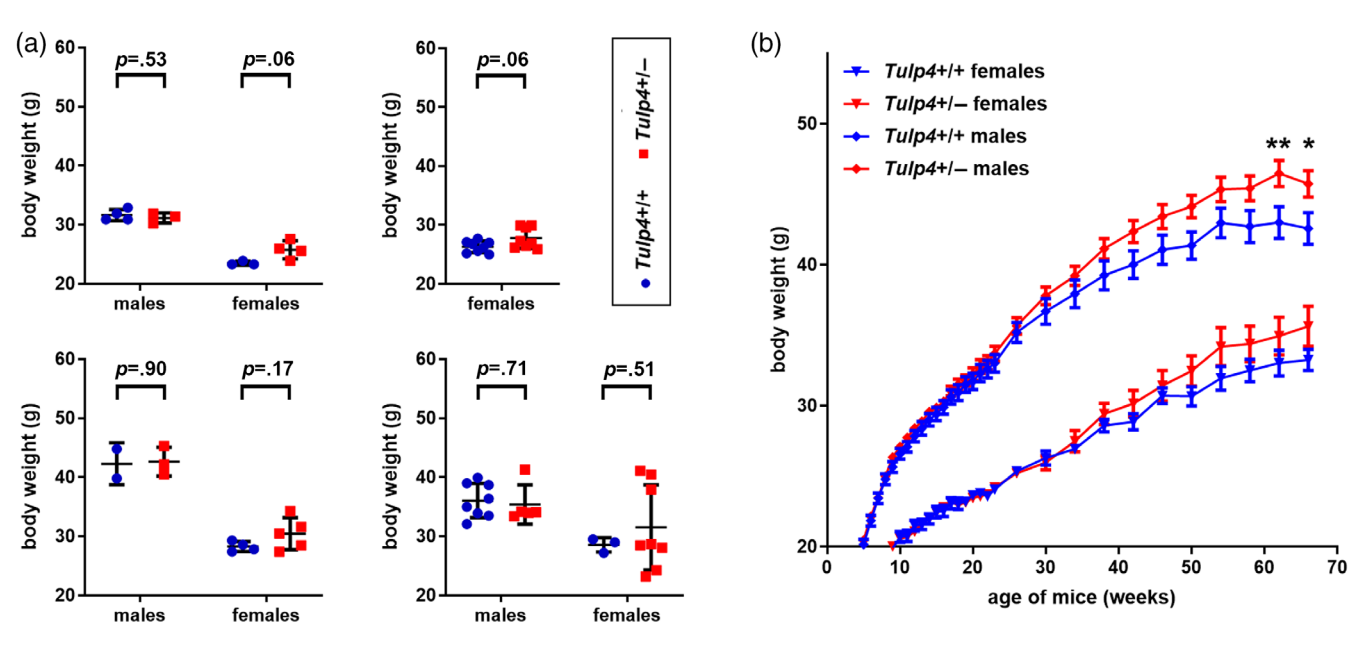


**FIGURE 6** Increased body weight observed in adult Tulp4+/- mice. (a) Spontaneous observations four independent cohorts suggest a trend for increased body weight in Tulp4+/- females aged 18 (upper left), 20 (lower left), 26 (upper right), and 31 (lower right) weeks. (b) Longitudinal weighting of a large mouse cohort (24 females and 40 males) under controlled conditions (four mice per cage; two Tulp4+/-, two Tulp4+/+) over a time span of 66 weeks. \*p < .05; \*p < .01.

controlled conditions. A total of 64 mice (24 females and 40 males), distributed into 16 cages (four mice per cage; two *Tulp4+/+*, and two *Tulp4+/-*) were maintained on standard diet, while body weight was measured at regular intervals over a total period of 66 weeks. Up to 23 weeks of age, we did not observe any weight differences neither for females nor for males. Upon further maintenance under standard conditions, a trend for increased body weight in *Tulp4+/-* mice became apparent at age 26 and 38 weeks for males and females, respectively (Figure 6b). These weight differences became increasingly pronounced when aging the mice up to 66 weeks of age. Notably, even though the initial spontaneous observations of genotype-specific weight differences were restricted to female mice, in the controlled weighting setup only the male group reached formal statistical significance at two time points (62 and 66 weeks of age). Nevertheless, the overall trend is apparent in both male and female cohorts (Figure 6b).

### 4 | DISCUSSION/CONCLUSION

Based on genetic association studies that suggested TULP4 as a candidate gene to influence risk of arterial thrombosis in patients with MPN, we have generated a knockout mouse model to study the effects of Tulp4 deficiency on hematopoiesis and beyond. While our phenotyping efforts did not reveal abnormalities in the hematopoietic system, it became apparent that systemic Tulp4 deficiency causes anatomic malformations in both Tulp4+/- and Tulp4-/- mouse embryos, subsequently resulting in perinatal lethality for the latter. This lethality phenotype presented at incomplete penetrance, which is a widespread phenomenon in mutant mouse lines observed

independently of the severity of malformations (Wilson et al., 2017). Interestingly, histopathological examinations of PO newborns revealed the presence of meconium in the large intestine of a nonviable Tulp4-/- newborn, indicative of a functional digestive system (Jerdee et al., 2015; Skelly et al., 2022). Subsequent anatomical examinations of both Tulp4-/- and Tulp4+/- embryos, using HREM in conjunction with classical histopathological examinations, identified a series of significant malformations on organ level that may be assigned to three different phenotypic classes: cardiac, vascular, and endocrine/exocrine gland-related (Figure 5). While the vascular phenotype is shared between Tulp4-/- and Tulp4+/-, observations of cardiac as well as endocrine/exocrine gland abnormalities were restricted to Tulp4-/- embryos. Although a causative involvement of endocrine or exocrine gland abnormalities such as abnormal thymus topology and small lobe or abnormal isthmus morphology of the thyroid gland in perinatal lethality cannot be excluded, the severe cardiac insufficiency caused by malformations, such as DORV, mVSD, and pVSD might primarily impact on the survival of Tulp4-/- embryos. Recent studies have shown that malformations of the cardiovascular system are often associated with abnormalities of the placenta (Camm et al., 2018; Courtney et al., 2018; Maslen, 2018; Perez-Garcia et al., 2018). Whether such placental defects are causal for the cardiovascular malformations detected in the Tulp4-/- embryos or whether they are directly responsible for embryonic lethality remains to be investigated. A series of minor, non-lethal malformations, and variants observed in Tulp4 deficient embryos was restricted to heterozygous Tulp4+/- mice, including organs and organ structures, such as muscles, lymphatic vessels, hypodermis, the nervous system, skeleton, and the reproductive system (Figure 5).

MICROSCOPY LWiley⊥ reference data for the developmental stages possibly present at E14.5 served for defining the "normal" morphology for each developmental stage actually observed at E14.5 (Geyer et al., 2022; Geyer, Reissig,

Despite the broad range of anatomic abnormalities detected in Tulp4+/- embryos, we did not find evidence for reduced birth rates of Tulp4+/- pups or reduced survival in Tulp4+/- adult mice. This might be explained by the benign nature of the defects and variants found in Tulp4+/- E14.5 embryos. Observed defects might be compatible with life, dissolve or become reduced in later embryonic or postnatal developmental stages. Alternatively, they might escape documentation in adult phenotyping efforts due to their persisting small size contained in the large volume of the mature organ. The latter possibility is supported by the absence of abnormal findings in our phenotyping efforts on Tulp4+/- adults, which included histopathological expert reviews of organs including heart, liver, bones, skin, as well as small blood vessels of relevant organs and large blood vessels as represented by the aorta. Extensive examinations of the hematopoietic system in conjunction with immunophenotyping of peripheral blood, bone marrow, and a number of relevant organ tissues (Supplementary Table S4) failed to establish connections with initial hypotheses derived from the genetic association studies on arterial thrombosis in MPN (Jäger et al., 2015), as no evidence for sporadic thrombosis was detected. While it was informative to examine blood parameters in the context of embryonic phenotyping, these basic analyses do not allow final conclusions on the role of TULP4 deficiency in MPN-related atherothrombosis. The latter condition results from an interplay of multifactorial causes (Hasselbalch et al., 2021: Libby et al., 2019; Moliterno et al., 2021; Sankar et al., 2019), none of which

has been specifically addressed in this work. From a technical point of view, considering the evidence for perinatal lethality in Tulp4-/- mice, we in a first step decided to apply classical histopathology methods to screen whole late-stage E17.5 embryos for the presence of anatomic abnormalities. Interestingly. histological analysis of 2D sections did not identify any of the macroanatomical malformations subsequently identified using HREM on E14.5 embryos. It is unlikely that superior detection rates on E14.5 embryos are based on the time difference between embryonic stages E14.5 and E17.5. One possible explanation would be that sagittal and parasagittal sections selected for light microscopic evaluation did not sufficiently capture defects existent in E17.5. While some of the defects identified by HREM might be generally visible also by histopathology, it remains a matter of randomness whether suitable sections exist and are selected for histopathological expert review. In contrary, HREM provides 3D volume data sets consisting of series of approximately 3000-4000 single images suited for comprehensive wholebody screens and volumetry. This resulted in the detection of anomalies in Tulp4-/- E14.5 embryos, and subsequently in Tulp4+/equivalents, which might have evaded classical 2D histological analysis. HREM has been employed as a key imaging method in the "Deciphering the mechanisms of developmental disorders" (DMDD) project, which aimed at detecting structural abnormalities in homozygous individuals of embryonic or perinatal lethal single knockout mouse lines at E14.5 (Mohun et al., 2013). For this reason, highly elaborated and standardized phenotyping protocols exist to enable systematic interrogation of embryos for malformations and subsequent annotation of

the detected phenotypes (Weninger et al., 2014). Moreover, detailed

Recent efforts to combine complementary imaging methodologies including classical histopathology and HREM demonstrated the advantages for multimodal analyses in respect of a simple 2D characterization of micro-anatomic morphologic defects (Keuenhof, Heimel, et al., 2021; Keuenhof, Kavirayani, et al., 2021; Walter et al., 2021; Zopf et al., 2021). Histopathology relies on tissue sections fixated on glass slides, followed by the acquisition of 2D images at certain magnifications, whereas HREM rather provides images from the surface of the block after cutting. Typically, HREM applies lower magnification to image larger areas as required for 3D modeling of whole embryos. In turn, classical histopathology has the potential to provide more detailed images on cellular and subcellular level in regions of interest. While in the Tulp4 knockout mouse model HREM showed superiority in detecting anomalies at a mesoscopic level, the correlative approach showcased herein generally has the potential to identify corresponding defects on cellular level, as frequently observed in mutant mouse models (Bolon, 2015; Rossant & Tam, 2007). Thus, exclusion of cellular lesions at the sites of anatomic anomalies in Tulp4-/- embryos (Figure 3) represents an important information in context of the observed phenotype.

Hüsemann, et al., 2017; Reissig et al., 2022).

Our observations on increased body weight in adult Tulp4+/mice (Figure 6) provide a notable phenotypic link between TULP4 and the TULP founding member TUB. In Tub mutant mice, obesity was reported to develop gradually, similar to late-onset obesity seen in humans. Tub mutant mice show increased body weight at an age of 15 weeks, subsequently reaching twice the weight of wildtype littermates (Coleman & Eicher, 1990). In contrast, increased weight in Tulp4+/- mice became apparent significantly later at an age of 26 weeks for males and 38 weeks for females (Figure 6). Moreover, weight differences between Tulp4+/- mice and their littermates appear rather mild as compared with weight gains in Tub mutant mice. Of note, the Tub-mediated obesity phenotype becomes obvious only in mice homozygous for the Tub mutation, nevertheless there is evidence for lipid-related phenotypes such as susceptibility for atherosclerosis also in heterozygous Tub mutant mice (Nishina et al., 1994a, 1994b). Recently, preliminary data on a mouse model carrying an endonuclease-mediated targeted Tulp4 allele (Tulp4<sup>em1(IMPC)Mbp</sup>) became available through the IMPC online database (https://www. mousephenotype.org/data/genes/; accession number MGI:1916092) (Groza et al., 2023). While a body weight phenotypic assay including such mice up to 17 weeks of age did not indicate genotypedependent weight differences (IMPC database as of February 27th, 2023), a potential weight phenotype later in life, as observed in our Tulp4 deficient mouse model, remains to be investigated. Of note, data presented on a viability primary screen (IMPC database as of February 27th, 2023) indicates preweaning lethality consequent to Tulp4 targeting, which is in line with the observations on our Tulp4—/— mice reported herein (Table 1).

Overall, by generating a novel mouse model of Tulp4 deficiency we could reveal and characterize a perinatal lethal phenotype in Tulp4-/- mice. We could further identify significant effects of Tulp4 deficiency on murine embryonic development in both Tulp4+/- and Tulp4-/- mice. Moreover, in adult Tulp4+/- we could identify a trend for increased body weight, which might link TULP4 to other TULP family members.

#### **AUTHOR CONTRIBUTIONS**

Roland Jäger: Conceptualization; investigation; writing - original draft; methodology; visualization; formal analysis; project administration; data curation; funding acquisition. Stefan Geyer H: Conceptualization; investigation; funding acquisition; writing - original draft; methodology; visualization; formal analysis; data curation. Anoop Kavirayani: Investigation; writing - original draft; methodology; formal analysis; data curation. Máté Kiss G: Investigation; writing - original draft; methodology; formal analysis. Elisabeth Waltenberger: Writing - review and editing; methodology; project administration; investigation. Thomas Rülicke: Writing - review and editing; investigation; methodology; resources. Christoph Binder J: Writing - review and editing; resources; methodology; investigation. Wolfgang J Weninger: Conceptualization; funding acquisition; writing - review and editing; methodology; supervision; resources; investigation. Robert Kralovics: Conceptualization; funding acquisition; investigation; writing - review and editing; methodology; supervision; resources.

### **ACKNOWLEDGMENTS**

The Tulp4 knockout mouse strain used for this research project was created from ES cell clone EPD0112 4 G12, obtained from the KOMP Repository (www.komp.org) and generated by the Wellcome Trust Sanger Institute (WTSI). Targeting vectors used were generated by the Wellcome Trust Sanger Institute and the Children's Hospital Oakland Research Institute as part of the Knockout Mouse Project (3U01HG004080). We thank Lill Kristin Andersen and Tina Bernthaler for their contribution to ES cell culture and mouse production, as well as Laura Göderle and Georg Obermayer for help with organ harvest and preparation. We would like to acknowledge Sarah Niggemeyer, Jenny Riede, and Sabine Jungwirth for animal caretaking. We further thank Agnieszka Piszczek, Tamara Engelmaier, and Julia Klughofer (all from the Histology Facility at Vienna BioCenter Core Facilities, member of the Vienna BioCenter (VBC)) for tissue processing and histochemical staining. The project benefitted from using Austrian BioImaging/CMI-facilities (https://www.bioimaging-austria.at/).

### **FUNDING INFORMATION**

This work was supported by Austrian Science Fund Projects F4702-B20 and P29018-B30 (R.K.).

### **CONFLICT OF INTEREST STATEMENT**

The authors declare no conflicts of interest statement.

### **DATA AVAILABILITY STATEMENT**

The data that support the findings of this study are available from the corresponding author upon reasonable request.

#### ORCID

Roland Jäger https://orcid.org/0000-0003-4530-1344

### **REFERENCES**

- Adams, D., Baldock, R., Bhattacharya, S., Copp, A. J., Dickinson, M., Greene, N. D. E., Henkelman, M., Justice, M., Mohun, T., Murray, S. A., Pauws, E., Raess, M., Rossant, J., Weaver, T., & West, D. (2013). Bloomsbury report on mouse embryo phenotyping: Recommendations from the IMPC workshop on embryonic lethal screening. *Disease Models & Mechanisms, dmm*.011833, 571–579. https://doi.org/10.1242/dmm.011833
- Banerjee, P., Kleyn, P. W., Knowles, J. A., Lewis, C. A., Ross, B. M., Parano, E., Kovats, S. G., Lee, J. J., Penchaszadeh, G. K., Ott, J., Jacobson, S. G., & Gilliam, T. C. (1998). TULP1 mutation in two extended Dominican kindreds with autosomal recessive retinitis pigmentosa. *Nature Genetics*, 18, 177–179. https://doi.org/10.1038/ng0298-177
- Bolon, B. (Ed.). (2015). Pathology of the developing mouse: A systematic approach. CRC Press. https://doi.org/10.1201/b18160
- Camm, E. J., Botting, K. J., & Sferruzzi-Perri, A. N. (2018). Near to one's heart: The intimate relationship between the placenta and fetal heart. Frontiers in Physiology, 9, 629. https://doi.org/10.3389/fphys.2018. 00629
- Coleman, D. L., & Eicher, E. M. (1990). Fat (fat) and tubby (tub): Two autosomal recessive mutations causing obesity syndromes in the mouse. *Journal of Heredity.*, 81, 424–427. https://doi.org/10.1093/oxfordjournals.jhered.a111019
- Courtney, J. A., Cnota, J. F., & Jones, H. N. (2018). The role of abnormal placentation in congenital heart disease; cause, correlate, or consequence? Frontiers in Physiology, 9, 1045. https://doi.org/10.3389/ fphys.2018.01045
- De Franco, E., Watson, R. A., Weninger, W. J., Wong, C. C., Flanagan, S. E., Caswell, R., Green, A., Tudor, C., Lelliott, C. J., Geyer, S. H., Maurer-Gesek, B., Reissig, L. F., Allen, H. L., Caliebe, A., Siebert, R., Holterhus, P. M., Deeb, A., Prin, F., Hilbrands, R., ... Barroso, I. (2019). A specific CNOT1 mutation results in a novel syndrome of pancreatic agenesis and holoprosencephaly through impaired pancreatic and neurological development. The American Journal of Human Genetics, 104, 985–989. https://doi.org/10.1016/j.ajhg.2019.03.018
- Geyer, S. H., Maurer-Gesek, B., Reissig, L. F., Rose, J., Prin, F., Wilson, R., Galli, A., Tudor, C., White, J. K., Mohun, T. J., & Weninger, W. J. (2022). The venous system of E14.5 mouse embryos—Reference data and examples for diagnosing malformations in embryos with gene deletions. *Journal of Anatomy*, 240, 11–22. https://doi.org/10.1111/joa.13536
- Geyer, S. H., Maurer-Gesek, B., Reissig, L. F., & Weninger, W. J. (2017). High-resolution episcopic microscopy (HREM)—Simple and robust protocols for processing and visualizing organic materials. *Journal of Visualized Experiments*, 125, 56701. https://doi.org/10.3791/56071
- Geyer, S. H., Reissig, L. F., Hüsemann, M., Höfle, C., Wilson, R., Prin, F., Szumska, D., Galli, A., Adams, D. J., White, J., Mohun, T. J., & Weninger, W. J. (2017). Morphology, topology and dimensions of the heart and arteries of genetically normal and mutant mouse embryos at stages S21-S23. *Journal of Anatomy*, 231, 600–614. https://doi.org/10.1111/joa.12663
- Geyer, S. H., Reissig, L., Rose, J., Wilson, R., Prin, F., Szumska, D., Ramirez-Solis, R., Tudor, C., White, J., Mohun, T. J., & Weninger, W. J. (2017). A staging system for correct phenotype interpretation of mouse embryos harvested on embryonic day 14 (E14.5). *Journal of Anatomy*, 230, 710–719. https://doi.org/10.1111/joa.12590
- Ghadge, S. K., Messner, M., Seiringer, H., Maurer, T., Staggl, S., Zeller, T., Müller, C., Börnigen, D., Weninger, W. J., Geyer, S. H., Sopper, S., Krogsdam, A., Pölzl, G., Bauer, A., & Zaruba, M. M. (2021). Smooth muscle specific ablation of CXCL12 in mice downregulates CXCR7

- associated with defective coronary arteries and cardiac hypertrophy. International Journal of Molecular Sciences, 22, 5908. https://doi.org/10.3390/iims22115908
- Groza, T., Gomez, F. L., Mashhadi, H. H., Muñoz-Fuentes, V., Gunes, O., Wilson, R., Cacheiro, P., Frost, A., Keskivali-Bond, P., Vardal, B., McCoy, A., Cheng, T. K., Santos, L., Wells, S., Smedley, D., Mallon, A. M., & Parkinson, H. (2023). The international mouse phenotyping consortium: Comprehensive knockout phenotyping underpinning the study of human disease. *Nucleic Acids Research*, 51, D1038–D1045. https://doi.org/10.1093/nar/gkac972
- Gu, S., Lennon, A., Li, Y., Lorenz, B., Fossarello, M., North, M., Gal, A., & Wright, A. (1998). Tubby-like protein-1 mutations in autosomal recessive retinitis pigmentosa. *The Lancet*, 351, 1103–1104. https://doi.org/10.1016/S0140-6736(05)79384-3
- Hagstrom, S. A., North, M. A., Nishina, P. M., Berson, E. L., & Dryja, T. P. (1998). Recessive mutations in the gene encoding the tubby-like protein TULP1 in patients with retinitis pigmentosa. *Nature Genetics*, 18, 174–176. https://doi.org/10.1038/ng0298-174
- Hasselbalch, H. C., Elvers, M., & Schafer, A. I. (2021). The pathobiology of thrombosis, microvascular disease, and hemorrhage in the myeloproliferative neoplasms. *Blood*, 137, 2152–2160. https://doi.org/10.1182/ blood.2020008109
- Jäger, R., Harutyunyan, A. S., Rumi, E., Gisslinger, B., Schalling, M., Ferretti, V., Pietra, D., Cazzola, M., Gisslinger, H., & Kralovics, R. (2015). Common variation at 6q25.3 (TULP4) influences risk for arterial thrombosis in myeloproliferative neoplasms. *Blood*, 126, 4088. https://doi.org/10.1182/BLOOD.V126.23.4088.4088
- Jerdee, T., Newman, B., & Rubesova, E. (2015). Meconium in perinatal imaging: Associations and clinical significance. Seminars in Ultrasound, CT and MRI, 36, 161–177. https://doi.org/10.1053/j.sult.2015.01.007
- Keuenhof, K., Heimel, P., Zopf, L. M., Raigel, M., Turyanskaya, A., Kavirayani, A., Reier, S., Glösmann, M., Schöfer, C., Kralovics, R., Streli, C., Weninger, W. J., Geyer, S. H., Slezak, P., Macfelda, K., Jäger, R., Wanek, T., & Walter, A. (2021). Multimodality imaging beyond CLEM: Showcases of combined in-vivo preclinical imaging and ex-vivo microscopy to detect murine mural vascular lesions. *Methods in Cell Biology*, 162, 389–415. https://doi.org/10.1016/bs.mcb.2020. 10.002
- Keuenhof, K. S., Kavirayani, A., Reier, S., Geyer, S. H., Weninger, W. J., & Walter, A. (2021). High-resolution episcopic microscopy (Hrem) in multimodal imaging approaches. *Biomedicines*, 9, 1918. https://doi.org/10.3390/biomedicines9121918
- Kleyn, P. W., Fan, W., Kovats, S. G., Lee, J. J., Pulido, J. C., Wu, Y., Berkemeier, L. R., Misumi, D. J., Holmgren, L., Charlat, O., Woolf, E. A., Tayber, O., Brody, T., Shu, P., Hawkins, F., Kennedy, B., Baldini, L., Ebeling, C., Alperin, G. D., ... Moore, K. J. (1996). Identification and characterization of the mouse obesity gene tubby: A member of a novel gene family. *Cell*, 85, 281–290. https://doi.org/10.1016/s0092-8674(00)81104-6
- Li, Q.-Z., Wang, C.-Y., Shi, J.-D., Ruan, Q.-G., Eckenrode, S., Davoodi-Semiromi, A., Kukar, T., Gu, Y., Lian, W., Wu, D., & She, J. X. (2001). Molecular cloning and characterization of the mouse and human TUSP gene, a novel member of the tubby superfamily. *Gene*, 273, 275–284. https://doi.org/10.1016/S0378-1119(01)00582-0
- Libby, P., Buring, J. E., Badimon, L., Hansson, G. K., Deanfield, J., Bittencourt, M. S., Tokgözoğlu, L., & Lewis, E. F. (2019). Atherosclerosis. *Nature Reviews Disease Primers*, 5, 56. https://doi.org/10.1038/s41572-019-0106-z
- Maslen, C. L. (2018). Recent advances in placenta-heart interactions. Frontiers in Physiology, 9, 735. https://doi.org/10.3389/fphys.2018.00735
- Mohun, T., Adams, D. J., Baldock, R., Bhattacharya, S., Copp, A. J., Hemberger, M., Houart, C., Hurles, M. E., Robertson, E., Smith, J. C., Weaver, T., & Weninger, W. (2013). Deciphering the mechanisms of developmental disorders (DMDD): A new programme for phenotyping

- embryonic lethal mice. *Disease Models & Mechanisms*, dmm.011957, 562–566. https://doi.org/10.1242/dmm.011957
- Mohun, T. J., & Weninger, W. J. (2012a). Embedding embryos for high-resolution Episcopic microscopy (HREM). Cold Spring Harbor Protocols, 2012, 678–680. https://doi.org/10.1101/pdb.prot069583
- Mohun, T. J., & Weninger, W. J. (2012b). Episcopic three-dimensional imaging of embryos. Cold Spring Harbor Protocols, 2012, 641–646. https://doi.org/10.1101/pdb.top069567
- Moliterno, A. R., Ginzburg, Y. Z., & Hoffman, R. (2021). Clinical insights into the origins of thrombosis in myeloproliferative neoplasms. *Blood*, 137, 1145–1153. https://doi.org/10.1182/blood.2020008043
- Mukhopadhyay, S., & Jackson, P. K. (2011). The tubby family proteins. *Genome Biology*, 12, 225. https://doi.org/10.1186/gb-2011-12-6-225
- Nishina, P. M., Lowe, S., Wang, J., & Paigen, B. (1994a). Characterization of plasma lipids in genetically obese mice: The mutants obese, Diabetes, Fat, Tubby, and Lethal Yellow. *Metabolism*, 43, 549–553.
- Nishina, P. M., Naggert, J. K., Verstuyft, J., & Paigen, B. (1994b). Atherosclerosis in genetically obese mice: The mutants obese, diabetes, fat, Tubby, and Lethal Yellow. *Metabolism*, 43, 554–558.
- Noben-Trauth, K., Naggert, J. K., North, M. A., & Nishina, P. M. (1996). A candidate gene for the mouse mutation tubby. *Nature*, 380, 534–538. https://doi.org/10.1038/380534a0
- North, M. A., Naggert, J. K., Yan, Y., Noben-Trauth, K., & Nishina, P. M. (1997). Molecular characterization of TUB, TULP1, and TULP2, members of the novel tubby gene family and their possible relation to ocular diseases. *Proceedings. National Academy of Sciences. United States of America*, 94, 3128–3133. https://doi.org/10.1073/pnas.94.7.3128
- Patterson, V. L., Damrau, C., Paudyal, A., Reeve, B., Grimes, D. T., Stewart, M. E., Williams, D. J., Siggers, P., Greenfield, A., & Murdoch, J. N. (2009). Mouse hitchhiker mutants have spina bifida, dorso-ventral patterning defects and polydactyly: Identification of Tulp3 as a novel negative regulator of the sonic hedgehog pathway. Human Molecular Genetics., 18, 1719–1739. https://doi.org/10.1093/hmg/ddp075
- Perez-Garcia, V., Fineberg, E., Wilson, R., Murray, A., Mazzeo, C. I., Tudor, C., Sienerth, A., White, J. K., Tuck, E., Ryder, E. J., Gleeson, D., Siragher, E., Wardle-Jones, H., Staudt, N., Wali, N., Collins, J., Geyer, S., Busch-Nentwich, E. M., Galli, A., ... Hemberger, M. (2018). Placentation defects are highly prevalent in embryonic lethal mouse mutants. *Nature*, 555, 463-468. https://doi.org/10.1038/nature26002
- Reissig, L. F., Geyer, S. H., Winkler, V., Preineder, E., Prin, F., Wilson, R., Galli, A., Tudor, C., White, J. K., Mohun, T. J., & Weninger, W. J. (2022). Detailed characterizations of cranial nerve anatomy in E14.5 mouse embryos/fetuses and their use as reference for diagnosing subtle, but potentially lethal malformations in mutants. Frontiers in Cell and Development Biology, 10, 1006620. https://doi.org/10.3389/fcell. 2022.1006620
- Rossant, J., & Tam, P. P. L. (2007). Mouse development: Patterning, morphogenesis, and organogenesis. Academic Press.
- Sankar, K., Stein, B. L., & Rampal, R. K. (2019). Thrombosis in the Philadel-phia chromosome-negative myeloproliferative neoplasms. In G. Soff (Ed.), Thrombosis and hemostasis in cancer cancer treatment and research (pp. 159–178). Springer International Publishing. https://doi.org/10.1007/978-3-030-20315-3\_11
- Skarnes, W. C., Rosen, B., West, A. P., Koutsourakis, M., Bushell, W., Iyer, V., Mujica, A. O., Thomas, M., Harrow, J., Cox, T., Jackson, D., Severin, J., Biggs, P., Fu, J., Nefedov, M., de Jong, P. J., Stewart, A. F., & Bradley, A. (2011). A conditional knockout resource for the genome-wide study of mouse gene function. *Nature*, 474, 337–342. https://doi.org/10.1038/nature10163
- Skelly, C. L., Zulfiqar, H., & Sankararaman, S. (2022). Meconium. In *Stat-Pearls*. StatPearls Publishing Available at: http://www.ncbi.nlm.nih.gov/books/NBK542240/ [Accessed November 14, 2022].

- Walter, A., Mannheim, J., & Caruana, C. J. (Eds.). (2021). *Imaging modalities* for biological and preclinical research. Volume 1. Part I, Ex vivo biological imaging: A compendium. Bristol [England]. IOP Publishing.
- Wang, M., Xu, Z., & Kong, Y. (2018). The tubby-like proteins kingdom in animals and plants. *Gene*, 642, 16–25. https://doi.org/10.1016/j.gene. 2017.10.077
- Wendling, O., Hentsch, D., Jacobs, H., Lemercier, N., Taubert, S., Pertuy, F., Vonesch, J. L., Sorg, T., di Michele, M., le Cam, L., Rosahl, T., Carballo-Jane, E., Liu, M., Mu, J., Mark, M., & Herault, Y. (2021). High resolution episcopic microscopy for qualitative and quantitative data in phenotyping altered embryos and adult mice using the new "Histo3D" system. *Biomedicine*, 9, 767. https://doi.org/10.3390/ biomedicines9070767
- Weninger, W. J., Geyer, S. H., Martineau, A., Galli, A., Adams, D. J., Wilson, R., & Mohun, T. J. (2014). Phenotyping structural abnormalities in mouse embryos using high-resolution episcopic microscopy. *Disease Models & Mechanisms*, 7, 1143–1152. https://doi.org/10. 1242/dmm.016337
- Weninger, W. J., Geyer, S. H., Mohun, T. J., Rasskin-Gutman, D., Matsui, T., Ribeiro, I., Costa, L. F., Izpisúa-Belmonte, J. C., & Müller, G. B. (2006). High-resolution episcopic microscopy: A rapid technique for high detailed 3D analysis of gene activity in the context of tissue architecture and morphology. *Anatomy and Embryology*, 211, 213–221. https://doi.org/10.1007/s00429-005-0073-x
- Weninger, W., Maurer-Gesek, B., Reissig, L., Prin, F., Wilson, R., Galli, A., Adams, D., White, J., Mohun, T., & Geyer, S. (2018). Visualising the cardiovascular system of embryos of biomedical model organisms with high resolution episcopic microscopy (HREM). *Journal of Cardiovascular Devel*opment and Disease, 5, 58. https://doi.org/10.3390/jcdd5040058

- Wilson, R., Geyer, S. H., Reissig, L., Rose, J., Szumska, D., Hardman, E., Prin, F., McGuire, C., Ramirez-Solis, R., White, J., Galli, A., Tudor, C., Tuck, E., Mazzeo, C. I., Smith, J. C., Robertson, E., Adams, D. J., Mohun, T., & Weninger, W. J. (2017). Highly variable penetrance of abnormal phenotypes in embryonic lethal knockout mice. Wellcome Open Research, 1, 1. https://doi.org/10.12688/wellcomeopenres. 9899.2
- Zopf, L. M., Heimel, P., Geyer, S. H., Kavirayani, A., Reier, S., Fröhlich, V., Stiglbauer-Tscholakoff, A., Chen, Z., Nics, L., Zinnanti, J., Drexler, W., Mitterhauser, M., Helbich, T., Weninger, W. J., Slezak, P., Obenauf, A., Bühler, K., & Walter, A. (2021). Cross-modality imaging of murine tumor vasculature—A feasibility study. *Molecular Imaging and Biology*, 23, 874–893. https://doi.org/10.1007/s11307-021-01615-y

#### SUPPORTING INFORMATION

Additional supporting information can be found online in the Supporting Information section at the end of this article.

How to cite this article: Jäger, R., Geyer, S. H., Kavirayani, A., Kiss, M. G., Waltenberger, E., Rülicke, T., Binder, C. J., Weninger, W. J., & Kralovics, R. (2024). Effects of *Tulp4* deficiency on murine embryonic development and adult phenotype. *Microscopy Research and Technique*, 87(4), 854–866. https://doi.org/10.1002/jemt.24476